BIOCHEMISTRY
including biophysical chemistry & molecular biology

Article

pubs.acs.org/biochemistry

Structural and Kinetic Insights into the "Ceftazidimase" Behavior of the Extended-Spectrum β-Lactamase CTX-M-96

Barbara Ghiglione,[†] María Margarita Rodríguez,[†] Raphaël Herman,[‡] Lucrecia Curto,[§] Milena Dropa,[∥] Fabrice Bouillenne,[‡] Frédéric Kerff,[‡] Moreno Galleni,[‡] Paulette Charlier,[‡] Gabriel Gutkind,[†] Eric Sauvage,[‡,⊥] and Pablo Power*[,†,⊥]

[†]Laboratorio de Resistencia Bacteriana, Facultad de Farmacia y Bioquímica and [§]IQUIFIB, Facultad de Farmacia y Bioquímica, Universidad de Buenos Aires, Buenos Aires, Argentina

[‡]Centre d'Ingéniérie des Protéines, Université de Liège, B-4000 Sart Tilman, Liège, Belgium

[∥]Faculdade de Saúde Pública, Universidade de São Paulo, São Paulo, Brazil

ABSTRACT: Diversification of the CTX-M β-lactamases led to the emergence of variants responsible for decreased susceptibility to ceftazidime, like the Asp240Gly-harboring "ceftazidimases". We solved the crystallographic structure of the Asp240Gly variant CTX-M-96 at 1.2 Å and evaluated the role of Asp240 in the activity toward oxyimino-cephalosporins through simulated models and kinetics. There seem to be subtle changes in the conformation of the active site cavity of CTX-M-96, compared to enzyme variants harboring the Asp240, and these small rearrangements could be due to localized shifts in the environment of the β3 strand. According to the crystallographic evidence, CTX-M-96 presents a "compact" active site, which in spite of its reduced cavity seems to allow the proper interaction with oxyimino-cephalosporins, as suggested by simulated models. The term "ceftazidimases" that is currently applied for the Asp240Gly-harboring CTX-M variants should be used carefully. Structural differences between CTX-M harboring the Asp240Gly mutation (and also probably others like those at Pro167) do not seem to be conclusive to determine the "ceftazidimase" behavior observed *in vivo*, which is in turn partially supported by the mild improvement in the catalytic efficiency toward ceftazidime by CTX-M-96 and similar enzymes, compared to "parental" Asp240-harboring variants. In addition, it is observed that alterations in OmpF expression could act synergistically with CTX-M-96 for yielding clinical resistance toward ceftazidime. We therefore propose that the observed resistance *in vivo* is due to the sum of synergic mechanisms, and the term "cefotaximases associated with ceftazidime resistance" could be conveniently used to describe CTX-M harboring the Asp240Gly substitution.

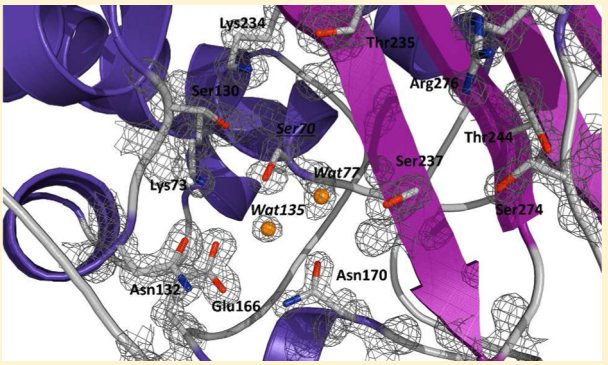

Since their initial identification, CTX-M β-lactamases represent today the most prevalent group of extended-spectrum β-lactamases (ESBL) among pathogens around the world.[1,2] These enzymes are highly prevalent in almost every country in which they are screened, for which they are currently considered as "pandemic β-lactamases".[3] At least five genetically distinct groups have been identified. They include over 150 assigned variants according to the Lahey's Web site (www.lahey.org/Studies). Among these variants, a considerable number of enzymes are encoded in the chromosome of *Kluyvera* species, a microorganism commonly found in the environment and sporadically isolated from clinical settings, from where the CTX-M β-lactamases have been apparently recruited as "preformed" genes by recombination and mobilization events and subsequently disseminated among pathogens.[2,4−7]

Acquired CTX-M are class A serine β-lactamases that confer high-level resistance to most β-lactams, including amino-penicillins, carboxy- and ureido-penicillins, and first- and second-generation cephalosporins. Regarding the oxyimino-(third generation) cephalosporins, CTX-M-producing organisms are generally resistant (or have elevated MICs) to cefotaxime or ceftriaxone, while ceftazidime usually remains in the susceptible range.[1] Stable substrates for which susceptibility is kept include the carbapenems and 7-α-methoxy-cephalosporins such as cefoxitin. As other class A β-lactamases, they are inhibited by mechanism-based β-lactamase inhibitors (clavulanate, sulbactam, and tazobactam).[8,9]

Compared to other ESBLs, CTX-M β-lactamases hydrolyze ceftazidime less effectively than cefotaxime,[9,10] due to a more favorable environment within the active site for the recognition and interaction for those substrates as compared to the bulky ceftazidime moiety.[11,12]

In this regard, diversification of the CTX-M β-lactamases has led to the emergence of variants that harbor mutations at key

Received: March 21, 2015
Revised: July 26, 2015
Published: July 30, 2015

DOI: 10.1021/acs.biochem.5b00313
Biochemistry 2015, 54, 5072−5082

amino acid positions that endorse the producing microorganisms with a decreased susceptibility to ceftazidime, probably as a result of an extensive use of ceftazidime in clinical settings.[2,8]

Among the amino acid substitutions present in these CTX-Ms, the Asp240Gly mutation is the most prevalent among the so-called "ceftazidimases",[11,13,14] resulting in an up to 8-fold increase in the MIC values for ceftazidime in the CTX-M producers.[15−17]

According to different studies on the structural properties of several CTX-M variants, the apparently improved hydrolytic efficiency of Asp240Gly mutants toward ceftazidime appears to be associated with a higher flexibility of the β3-strand, although this substitution is also correlated with lower stability.[11] Recent studies revealed "breathing" of CTX-M β-lactamases and the implication that the Asp240Gly replacement accommodated ceftazidime more efficiently.[18] Other factors like "covalent trapping" phenomena have been suggested as responsible for ceftazidime resistance in other β-lactamases,[19−21] although it seems unlikely for the CTX-M.

Other mutations were also implicated in a higher "ceftazidimase" activity. Mutations at Pro167, occurring in the immediate vicinity of the Ω loop, apparently modify the interaction with the oxyimino-cephalosporin.[22] Nevertheless, even when mutations that occur in these positions generally lead to large increases in the MICs to ceftazidime for the producing strains, only discrete catalytic efficiency toward ceftazidime is obtained.[2,8] Moreover, it has also been noted that Asp240Gly substitutions have been selected more frequently than mutations in Pro167, probably because modifications in residues comprising the Ω-loop result in a significant decrease in the catalytic efficiencies.[2] In this regard, it is noteworthy that the evolution of CTX-M enzymes along the Pro167 pathway has limited possibilities of further diversification, while the Asp240 route has a more robust diversification which is favored in the simultaneous presence of both cefotaxime and ceftazidime selective forces.[23]

Among the main objectives pursued in this work, we studied the crystallographic structure of the natural Asp240Gly mutant CTX-M-96, that belongs to the CTX-M-1/3 cluster, evaluated the actual role of Asp240 in the activity toward oxyimino-cephalosporins through simulated models, and, finally, present some additional insights to explain the influence of other factors in the overall resistance to ceftazidime in CTX-M-producing bacteria.

EXPERIMENTAL PROCEDURES

Bacterial Strains and Plasmids. *Klebsiella pneumoniae* 293235 was used as source of the $bla_{CTX\text{-}M\text{-}96}$, deposited as $bla_{CTX\text{-}M\text{-}12a}$ and lately renumbered to fulfill the current functional classification scheme (www.lahey.org/Studies).[24,25] *K. pneumoniae* 1338 is a clinical isolate used as source of plasmid-borne $bla_{CTX\text{-}M\text{-}12}$.[25] *Escherichia coli* ATCC 25922 strain was used as quality control strain for antimicrobial susceptibility assays.[26] *E. coli* XL1-Blue (Stratagene, USA) and *E. coli* BL21(DE3) (Novagen, USA) were hosts for transformation experiments.

E. coli K12 and derived isogenic strains with alterations in the level of different major outer membrane proteins (Omp) were used to assess the influence of porin's deficiency in the overall resistance profile, as described:[27] *E. coli* JF700 (*ompF*$^-$, *ompA*$^-$), *E. coli* JF701 (*ompC*$^-$), *E. coli* JF703 (*ompF*$^-$), and *E. coli* JF694 (*ompF*$^-$, *ompC*$^-$). These strains were generously obtained from the *E. coli* Genetic Stock Center (CGSC, Yale University).

Plasmid DNA from *K. pneumoniae* 293235 (pKpn235) and *K. pneumoniae* 1338 (pKpn38) were extracted by the Hansen-Olsen methodology.[28] Plasmid vectors pTZ57R/T (InsTA-clone PCR Cloning kit, Thermo Scientific, USA), pK19,[29] and kanamycin-resistant pET28a(+) (Novagen, Germany) were used for routine cloning experiments and as production vectors.

Antibiotic Susceptibility. Antimicrobial susceptibility was evaluated for clinical isolates and recombinant *E. coli* clones, by a disk diffusion method and by determination of the minimum inhibitory concentrations (MICs), according to current CLSI's guidelines.[26]

Recombinant DNA Methodologies. For those methodologies in which expression of $bla_{CTX\text{-}M}$ genes was achieved from the pK19 vector, CTX-M-96 and CTX-M-12 encoding genes were amplified by PCR from plasmids pKpn235 and pKpn38, using 3 U PrimeSTAR HS DNA polymerase (Takara, USA), and 1 μM of primers CTX-M-1 FpK (5′-AAATG-GTTAAAAAATCACTGC-3′) and CTX-M-1 RpK (5′-CTACAAACCGTCGGTGACGAT-3′). PCR-products were cloned at the *Sma*I site of the pK19 vector, and transformed in competent *E. coli* XL1BLUE, to yield recombinant plasmids pK12 and pK96 expressing CTX-M-12 and CTX-M-96, respectively.

For cloning the $bla_{CTX\text{-}M}$ genes in vectors that allow their overexpression, PCR were performed using plasmids pKpn235 and pKpn38 as templates, 3 U PrimeSTAR, and 1 μM of primers PFNcoGPO1 (5′-CCATGGTTAAAAAATCAC-TGCGCC-3′) and PRHind3GPO1 primers (5′-AAGCTT-ACAAACCGTCGGTGACG-3′) containing the *Nco*I and *Hin*dIII restriction sites, respectively (underlined in the sequences), to allow the cloning of the wild-type CTX-M-96 coding sequence; for cloning wild-type CTX-M-12 coding gene, primer PFNdeG1p28Ht (5′-CTGCATATGCAAACGG-CGGACG-3′) including the *Nde*I restriction site (underlined) was used instead of the PFNcoGPO1 primer. PCR products were first ligated in a pTZ57R/T vector, and the insets were sequenced for verification of the identity of $bla_{CTX\text{-}M}$ genes and generated restriction sites, as well as the absence of aberrant nucleotides. Resulting recombinant plasmids (pFMT12 and pFMT96) were then digested with *Nco*I and *Hin*dIII (for $bla_{CTX\text{-}M\text{-}96}$), or *Nde*I and *Hin*dIII (for $bla_{CTX\text{-}M\text{-}12}$), and the released inserts were subsequently purified and cloned in the *Nco*I-*Hin*dIII or *Nde*I-*Hin*dIII sites of a pET28a(+) vector, as appropriate. Ligation mixtures were used to first transform *E. coli* XL1-Blue competent cells, and after selection of recombinant clones, a second transformation was performed in *E. coli* BL21(DE3) competent cells in LBA plates supplemented with 30 μg mL^{-1} kanamycin. Selected positive recombinant clones were sequenced to confirm the identity of the $bla_{CTX\text{-}M}$ genes, and recombinant clones harboring the resulting pET12 and pET96 plasmids were obtained for protein expression experiments.

DNA sequences were determined at Macrogen Inc. (South Korea). Nucleotide and amino acid sequence analyses were conducted by NCBI (http://www.ncbi.nlm.nih.gov/) and ExPASy (http://www.expasy.org/) analysis tools.

Determination of β-Lactamase Activity. Crude lysates from overnight cultures of *E. coli* XL1Blue harboring either pK12 or pK96 plasmids (expressing $bla_{CTX\text{-}M\text{-}12}$ or $bla_{CTX\text{-}M\text{-}96}$, respectively) were obtained as described before.[30]

DOI: 10.1021/acs.biochem.5b00313
Biochemistry 2015, 54, 5072−5082

β-Lactamase activity was determined spectrophotometrically by measuring the hydrolysis of 100 μM cephalothin as substrate (λ = 273 nm; $\Delta\varepsilon$M = −6300 M^{-1} cm^{-1}). One unit of β-lactamase activity (U) was defined as the amount of enzyme which hydrolyses 1 nmole of substrate per minute (in 20 mM phosphate buffer, pH 7.0) at 30 °C. The specific activity was defined as the units of β-lactamase per milligram of protein, determined by the BioRad Protein Assay kit (BioRad, USA).

Production and Purification of CTX-M-96 and CTX-M-12. Overnight cultures of recombinant *E. coli* BL21 clones producing CTX-M-96 and CTX-M-12 were diluted (1/400) in 1.75 L LB containing 30 μg mL^{-1} kanamycin and grown at 37 °C until ca. 0.6 OD units (λ = 600 nm). In order to induce β-lactamase expression, 1 mM IPTG was added, and cultures were grown at 28 °C during 3.5 h. After centrifugation at 8000 rpm for 20 min (4 °C) in a Sorvall RC-5C (GS3 rotor), cells were resuspended in the corresponding buffer.

For *E. coli* 96B (harboring pET96 plasmid), cells were resuspended in 50 mM MES buffer (pH 6.5; buffer A), and crude extracts were obtained by mechanic disruption in an EmulsiFlex-C3 homogenizer (Avestin Europe GmbH, Germany) after three passages at 1500 bar. After clarification by centrifugation at 19 000 rpm for 20 min (4 °C, SS34 rotor), clear supernatants containing the CTX-M-96 β-lactamase were dialyzed overnight against 10 L buffer A. Clear supernatants were filtrated by 0.7 and 0.45 μm pore size membranes and loaded onto a 24 mL SP Sepharose HP column (GE Healthcare Europe GmbH, Belgium), connected to an ÄKTA-purifier (GE Healthcare, Uppsala, Sweden), and equilibrated with buffer A. The column was extensively washed to remove unbound proteins, and β-lactamases were eluted with a linear gradient (0−60%; 3 mL min^{-1} flow rate) of buffer B: buffer A + 1 M NaCl. Eluted fractions were screened *in situ* for β-lactamase activity during purification by nitrocefin hydrolysis, and confirmed by SDS-PAGE in 12% polyacrylamide gels. Active fractions were pooled and dialyzed against buffer A, and loaded onto a Mono-S 5/50 GL column (GE Healthcare Europe GmbH, Belgium) equilibrated in buffer A, and pure mature CTX-M-96 was eluted with a linear gradient (0−30%; 1 mL min^{-1} flow rate) of buffer B.

For *E. coli* 12B (harboring pET12 plasmid), cells were resuspended in 50 mM Tris/200 mM NaCl buffer (pH 8.0; buffer A), and crude extracts were obtained by mechanic disruption in a Vibra Cell sonicator (Sonics & Materials Inc., USA). After clarification by centrifugation at 13 000 rpm for 20 min (4 °C, SS34 rotor), clear supernatants containing the CTX-M-12 β-lactamase were dialyzed overnight against 10 L buffer A. Clear supernatants were filtrated by 0.45 μm pore size membranes and loaded onto a 5 mL HisTrap HP column (GE Healthcare Europe GmbH, Belgium), connected to an ÄKTA-purifier (GE Healthcare, Uppsala, Sweden), and equilibrated with buffer A. The column was extensively washed to remove unbound proteins, and β-lactamases were eluted with a linear gradient (0−60%; 2 mL min^{-1} flow rate) of buffer B: buffer A + 500 mM imidazol. Eluted fractions were screened for β-lactamase activity *in situ* during purification by nitrocefin hydrolysis and confirmed by SDS-PAGE in 12% polyacrylamide gels. Active fractions were pooled and dialyzed overnight against buffer PBS. Thrombin digestion (GE Healthcare Life Sciences, USA) was performed at 16 °C to remove the histidine tag, according to manufacturer's indications. Eluted proteins were conserved at −70 °C until use. Protein concentration and purity were determined by the BCA-protein quantitation assay (Pierce, Rockford, IL, US) using bovine serum albumin as standard, and by densitometry analysis on 15% SDS-PAGE gels, respectively.

Kinetics. Steady-state kinetic parameters were determined using a T80 UV/vis spectrophotometer (PG Instruments Ltd., UK). Each reaction was performed in a total volume of 500 μL at room temperature. The steady-state kinetic parameters K_M and V_{max} were obtained under initial-rate as described previously,[31] with nonlinear least-squares fitting of the data (Henri Michaelis−Menten equation) using GraphPad Prism 5.03 for Windows (GraphPad Software, San Diego California USA):

$$v = (V_{max} \times [S])/(K_M + [S]) \quad (1)$$

For low K_M values, the k_{cat} values were derived by evaluation of the complete hydrolysis time courses as described by De Meester et al.[32] For competitive inhibitors, inhibition constant K_I (as $K_{I\,obs}$) was determined by monitoring the residual activity of the enzyme in the presence of various concentrations of the drug and 100 μM cephalothin as reporter substrate; corrected K_I (considered as the observed or apparent K_M) value is finally determined using the equation:

$$K_I = K_{I\,obs}/(1 + [S]/K_{M(S)}) \quad (2)$$

where $K_{M(S)}$ and [S] are the reporter substrate's K_M and fixed concentration used, respectively.

For irreversible inhibitors, the rate constant of inactivation, k_{inact}, was measured directly by time-dependent inactivation of CTX-M in the presence of the inhibitor, using a fixed concentration of enzyme and 100 μM nitrocefin as reporter, and increasing concentrations of the inhibitor. The observed rate constant for inactivation (k_{obs}) was determined by nonlinear least-squares fitting of the data using OriginPro 8.0 (Northampton, MA, USA), using the eq 3, as described elsewhere.[33]

$$A = A_0 + v_f \times t + (v_0 - v_f) \times [1 - \exp(-k_{obs} \times t)]/k_{obs} \quad (3)$$

Then, k_{obs} values were plotted against the inhibitor concentration, and inactivation constant, k_{inact}, was obtained by nonlinear fitting of the eq 4, using GraphPad Prism:

$$k_{obs} = (k_{inact} \times [I])/(K_M + [I]) \quad (4)$$

The following extinction coefficients and wavelengths were used:[34] benzyl-penicillin ($\Delta\varepsilon_{235}$ = −775 M^{-1} cm^{-1}), ampicillin ($\Delta\varepsilon_{235}$ = −820 M^{-1} cm^{-1}), piperacillin ($\Delta\varepsilon_{235}$ = −820 M^{-1} cm^{-1}), cephalothin ($\Delta\varepsilon_{273}$ = −6300 M^{-1} cm^{-1}), cefuroxime ($\Delta\varepsilon_{260}$ = −7600 M^{-1} cm^{-1}), cefoxitin ($\Delta\varepsilon_{260}$ = −6600 M^{-1} cm^{-1}), ceftazidime ($\Delta\varepsilon_{260}$ = −9000 M^{-1} cm^{-1}), cefotaxime ($\Delta\varepsilon_{260}$ = −7500 M^{-1} cm^{-1}), cefepime ($\Delta\varepsilon_{260}$ = −10 000 M^{-1} cm^{-1}), imipenem ($\Delta\varepsilon_{300}$ = −9000 M^{-1} cm^{-1}), and aztreonam ($\Delta\varepsilon_{318}$ = −750 M^{-1} cm^{-1}).

Crystallization of CTX-M-96. Crystals were grown at 20 °C by hanging drop vapor diffusion with drops containing 0.2 μL of CTX-M-96 solution (15 mg mL^{-1}) and 0.2 μL of ammonium citrate 2 M in 0.1 M bis-tris propane buffer (pH 7.0), equilibrated against 1 mL of the latter solution at 20 °C.

Data Collection, Phasing, Model Building and Refinement. Data were collected at 100 K on an ADSC Q315r CCD detector at a wavelength of 0.98011 Å on Proxima 1 beamline at the Soleil Synchrotron (Saint Aubin, France). Indexing and

DOI: 10.1021/acs.biochem.5b00313
Biochemistry 2015, 54, 5072−5082

Table 1. Minimum Inhibitory Concentrations (MIC, in μg mL^{-1}) of Parental Isolates and Recombinant Clones

antibiotic	*K. pneumoniae* 293235 ($bla_{CTX-M-96}$)	*E. coli* XL1Blue (pK96)	*K. pneumoniae* 1338 ($bla_{CTX-M-12}$)	*E. coli* XL1Blue (pK12)	*E. coli* XL1Blue	*E. coli* XL1Blue (pK19)
ampicillin	>256	>1024	>256	>1024	2	2
piperacillin	>256	>256	>256	>256	1	1
piperacillin + tazobactam	ND	2	ND	2	0.5	0.5
cephalothin	>1024	>1024	>1024	>1024	2	4
cefotaxime	>256	256	128	128	≤0.125	≤0.125
cefotaxime + clavulanic acid	2	≤0.125	2	≤0.125	≤0.125	≤0.125
ceftazidime	>256	8	64	1	≤0.125	≤0.125
ceftazidime + clavulanic acid	2	≤0.125	2	≤0.125	≤0.125	≤0.125
cefepime	32	4	64	8	≤0.125	≤0.125
cefoxitin	4	2	8	2	2	2
imipenem	0.5	≤0.125	0.5	≤0.125	≤0.125	≤0.125

Table 2. Comparative Steady-State Kinetic Parameters of CTX-M-96 and CTX-M-12 β-Lactamases[a]

	CTX-M-96			CTX-M-12			
β-lactam substrate	k_{cat} (s^{-1})	K_M (μM)	k_{cat}/K_M (μM^{-1} s^{-1})	k_{cat} (s^{-1})	K_M (μM)	k_{cat}/K_M (μM^{-1} s^{-1})	efficiency factor[c]
benzyl-penicillin[b]	37 ± 1.0	4.0 ± 0.1	9.3 ± 0.5	nd	nd		
ampicillin[b]	23 ± 1.0	5.0 ± 0.2	4.6 ± 0.3	130 ± 4.0	5.0 ± 0.1	26 ± 1.0	0.18
piperacillin[b]	38 ± 2.0	1.0 ± 0.1	38 ± 6.0	nd	nd		
cephalothin	120 ± 4.0	27 ± 3.0	4.4 ± 0.7	970 ± 68	130 ± 5.0	7.5 ± 0.8	0.59
cefuroxime	45 ± 3.0	17 ± 3.0	2.6 ± 0.7	nd	nd		
cefoxitin[b]	$3 \times 10^{-4} \pm 5 \times 10^{-5}$	50 ± 4	$6 \times 10^{-6} \pm 1 \times 10^{-6}$	nd	nd		
cefotaxime	60.0 ± 2.4	34 ± 2.0	1.8 ± 0.2	78 ± 4.0	44 ± 3.0	1.8 ± 0.2	1
ceftazidime[b]	4 ± 1	1400 ± 250	0.003 ± 0.0001	1.0 ± 0.3	1660 ± 464	$6 \times 10^{-4} \pm 6 \times 10^{-6}$	5
cefepime	30 ± 6	607 ± 144	0.05 ± 0.02	80 ± 9	570 ± 17	0.14 ± 0.02	0.36
aztreonam	0.90 ± 0.05	46 ± 2.8	0.02 ± 0.01	8.0 ± 0.2	170 ± 10	0.05 ± 0.004	0.4
imipenem[b]	$0.0013 \pm 9 \times 10^{-5}$	71 ± 6	$2 \times 10^{-5} \pm 5 \times 10^{-6}$	nd	nd		
inhibitors	k_{inact} (s^{-1})	K_I (μM)	k_{inact}/K_I (μM^{-1} s^{-1})	k_{inact} (s^{-1})	K_I (μM)	k_{inact}/K_I (μM^{-1} s^{-1})	
clavulanic acid	0.03 ± 0.002	0.67 ± 0.07	0.045 ± 0.007	nd	nd		
tazobactam	0.095 ± 0.006	0.43 ± 0.04	0.22 ± 0.04	0.11 ± 0.01	0.035 ± 0.002	3.2 ± 0.13	

[a]nd: not determined. [b]K_M constants were determined as K_I obs by competitive assays with reporter substrates (see Experimental Procedures). [c]Efficiency factor: ratio between k_{cat}/K_M of Gly240 mutant CTX-M-96 vs Asp240 wild type CTX-M-12 β-lactamases.

integration were carried out using XDS,[35] and the scaling of the intensity data was accomplished with XSCALE.[36]

Refinement of the model was carried out using REFMAC5,[37] TLS,[38] and Coot.[39] Models visualization and representation were performed with PyMol (www.pymol.org).[40] The structure of CTX-M-96 β-lactamase was refined to 1.2 Å, and deposited at the Protein Data Bank (PDB) under accession code 3ZNY.

Sequence and structural alignments were also performed using T-Coffee Expresso[41] and ESPript/ENDscript.[42]

Simulated Modeling of CTX-M-96 in Complex with Oxyimino-Cephalosporins and Clavulanate. The X-ray structure of CTX-M-96 was used to model acyl-enzyme structures with ceftazidime, cefotaxime, and clavulanic acid. The structures with PDB code 2ZQD (TOHO-1 in complex with ceftazidime), 1IYO (TOHO-1 in complex with cefotaxime[43]), and 2H0T (SHV-1 in complex with clavulanic acid[44]) were used for initial positioning of each ligand in CTX-M-96 structure. Simulation structures were energy minimized with the program Yasara,[45] using a standard protocol that consists of the steepest descent minimization followed by simulated annealing of the ligand and protein side chains. CTX-M-96 backbone atoms were kept fixed during the whole procedure. Simulation parameters consisted of the use of Yasara2 force field,[46] a cutoff distance of 7.86 Å, particle mesh Ewald (PME) long-range electrostatics,[47] periodic boundary conditions, and water filled simulation cell.

Circular Dichroism. Spectra were recorded on a Jasco J-810 spectropolarimeter. Data in the near UV (250−320 nm) or in the far UV (200−250 nm) regions were collected at 25 °C using 10 or 1 mm path length cuvettes, respectively. A scan speed of 20 nm min^{-1} with a time constant of 1 s was used for both proteins. Each spectrum was measured at least three times, and the data were averaged to minimize noise. Molar ellipticity was calculated as described elsewhere,[48] using a mean residue weight value of 107.

Fluorescence Measurements. Fluorescence measurements were performed at 25 °C in a Jasco FP-6500 spectrofluorimeter equipped with a thermostated cell. A 3 mm path cuvette sealed with a Teflon cap was used. The excitation wavelength was 295 nm, and emission was collected in the range 300−410 nm. The excitation and emission monochromator slit widths were both set at 3 nm.

Transformation in Omp-Deficient *E. coli* Strains. Chemically competent cells of *E. coli* K12 and isogenic *Omp*-deficient strains were obtained by standard protocols and used as recipients for heat-shock transformation with plasmids pK12 and pK96, that harbor $bla_{CTX-M-12}$ and $bla_{CTX-M-96}$, respectively. Controls were included, using empty pK19 vector as donor

DOI: 10.1021/acs.biochem.5b00313
Biochemistry 2015, 54, 5072−5082

DNA. Positive transformant clones were selected in LBA plates supplemented with 30 μg mL^{-1} kanamycin, and the presence of the plasmid was verified by plasmid DNA extraction and visualization in 0.8% agarose gels.

RESULTS AND DISCUSSION

CTX-M-96 Confers Reduced Susceptibility to Ceftazidime. As observed in Table 1, both *K. pneumoniae* isolates displayed an antimicrobial susceptibility profile compatible with an ESBL producer, including resistance to both cefotaxime and ceftazidime. Only after the $bla_{CTX\text{-}M}$ genes were cloned in a suitable vector, and expressed from an *E. coli* strain, we observed the differential behavior of other CTX-M producers: the *E. coli* clone harboring the pK96 recombinant plasmid presented an 8-fold increase in the MIC of ceftazidime compared to the clone producing CTX-M-12 (harboring plasmid pK12), although insufficient to yield clinical resistance to the drug. These differences in MIC values do not seem to be the result of different levels of enzyme production between both clones, because specific activities against cephalothin were equivalent (35 and 40 U mg^{-1} for *E. coli* harboring pK12 and pK96, respectively).

This behavior is equivalent to other reported enterobacteria isolates that produce CTX-M β-lactamases: most of the CTX-M producers are resistant to cefotaxime and remain susceptible to ceftazidime, and a reduced susceptibility to the latter is observed in isolated producing variants of CTX-M β-lactamases,[1,2] Among these variants, the most prevalent mutations are those that occur at positions 240 (the mutation Asp240Gly), mainly selected by *in vivo* treatment with ceftazidime,[8] and at Pro167.[22]

CTX-M-96 Is a Natural Asp240Gly Mutant That Displays Only Discrete Increases in the Activity toward Ceftazidime. CTX-M-96 shows the highest catalytic efficiencies (k_{cat}/K_M) toward penicillins, first and second generation cephalosporins, and cefotaxime (Table 2). We named an "efficiency factor" (EF) as the ratio between the catalytic efficiencies of CTX-M-96 and CTX-M-12, respectively, toward a specific β-lactam. For ceftazidime, the EF is 5, being the highest value among the substrates compared. In fact, except for cefotaxime, for which the k_{cat}/K_M remains invariant (1.8 μM^{-1} s^{-1}), for the other substrates the catalytic efficiency clearly diminishes and yields EF between 0.18 and 0.59. Nevertheless, even when CTX-M-96 displays a 5-fold increase in the catalytic efficiency toward ceftazidime compared to CTX-M-12, it remains 600-fold lower than that for cefotaxime: 0.003 vs 1.8 μM^{-1} s^{-1}, respectively (Table 2). This behavior is due to flagrant differences in the steady state parameters; while cefotaxime is turned over 15-fold faster than ceftazidime (k_{cat} = 60 vs 4 s^{-1}), the affinity of both oxyimino-cephalosporins for the CTX-M-96 active site is about 40-fold higher in favor of cefotaxime against ceftazidime (K_M = 34 vs 1400 μM, respectively). Although our values are different from those determined by Bae et al.,[49] there is agreement in the comparative behavior of both enzymes toward ceftazidime.

By competitive assays between ceftazidime and nitrocefin, we could not observe significant inhibition of both CTX-M-96 and CTX-M-12 even after using up to 5 mM ceftazidime, confirming that K_M for ceftazidime reaches values in the millimolar range (data not shown). We also performed precompetitive assays in which we incubated the enzyme with increasing concentrations of ceftazidime, and a slight inhibition was observed only after at least 2 h preincubation (data not shown). These results suggest that efficient hydrolysis of ceftazidime could only occur with either high concentrations of ceftazidime in the medium and/or after prolonged incubation times with the enzyme, two conditions that can hardly be accomplished during *in vivo* treatments.

As stated before, the hydrolytic efficiencies toward most of the substrates assayed were noticeably lower for the Asp240Gly mutant CTX-M-96 than the wild type CTX-M-12. As observed in Table 2, efficiency factors for ampicillin, cephalothin, cefepime, and aztreonam (0.18, 0.59, 0.36, and 0.4, respectively) suggest that CTX-M-96 pays some cost to gain some activity toward ceftazidime by losing hydrolytic efficiency toward these other substrates. In fact, the Asp240Gly mutation does not seem to have a deleterious impact in the overall resistance phenotype of CTX-M-96 producing *E. coli* clones, as observed in Table 1; both CTX-M-12 and CTX-M-96 producers remain resistant to penicillins, and first and second generation cephalosporins, and only MIC of ceftazidime increases 8-fold in the Asp240Gly mutant.

CTX-M-96 also showed an efficient inhibition by both clavulanic acid and tazobactam, the latter being a more potent inhibitor. The Asp240Gly mutation also impairs the ability of mechanism-based inhibitors to block the β-lactamases; for tazobactam, CTX-M-96 appears to be almost 15-fold less efficiently inhibited than CTX-M-12 (k_{inact}/K_I = 0.22 vs 3.2 μM^{-1} s^{-1}, respectively).

Structure Determination of CTX-M-96 β-Lactamase. The refined structure of CTX-M-96 (previously known as CTX-M-12a; UniProt identifier Q6ZXB6) was obtained at high resolution (1.20 Å). Main data and refinement statistics are given in Table 3.

The refined structure consists of one monomer per asymmetric unit. The electron density map is well-defined along the main chain. The amino acid numbering scheme used in this structure follows the Ambler's consensus system.[50] The monomer includes 260 amino acids of mature β-lactamase, from Asp28 to Leu290. Mature CTX-M-96 contains 263 residues, for which 98% of total residues were observed in the structure (only the three first residues of the mature chain, Gln25-Thr26-Ala27, were not observed). The structure is solvated by 384 ordered water molecules. The average occupancy-weighted temperature factor was 11.1 Å^2 (±5.4 Å^2), close to the value estimated by the Wilson plot (14.7 Å^2).[51]

Most Relevant Structural Features of CTX-M-96 and Comparison with Other Class A β-Lactamases. The overall fold of the native CTX-M-96 β-lactamase is similar to previously reported CTX-M enzymes. Also, the catalytic cleft is located in the junction between the main "all α" and "α/β" domains, a typical structural signature from all studied class A β-lactamases.[52]

The root-mean-square deviations (rmsd) values for Cα atoms between the main chain of CTX-M-96 with different CTX-Ms and other class A β-lactamases were determined. Root-mean-square deviations in some specific regions such as the Ω loop and β3 strand are in agreement with the previously reported increased flexibility in these domains.[11,53] On the other hand, regions that cover the active-site motifs have very low rmsd values, according to the high conservation of these domains necessary for the proper conformation of the active site (Table 4).

Even when the rmsd values for the Ω loop among the CTX-M structures are generally low, the highest degree of conservation was observed with CTX-M-15, which is clustered

DOI: 10.1021/acs.biochem.5b00313
Biochemistry 2015, 54, 5072−5082

Table 3. Data Collection, Diffraction, and Phasing Statistics for Native CTX-M-96 β-Lactamase

parameter	value[a]		
crystal	native CTX-M-96		
PDB code	3ZNY		
Data collection:			
space group	*P* 21 21 21		
cell parameters (Å)	*a* = 44.57	*b* = 45.59	*c* = 117.40
	α = 90.00	*β* = 90.00	*γ* = 90.00
average mosaicity	0.07		
subunits/asu	1		
resolution range (Å)	45.59−1.20 (1.26−1.20)		
number of unique reflections	75509 (68527)[b]		
R_{merge} (%)	4.8 (29.2)		
redundancy	11.9 (7.4)		
completeness (%)	98.8 (91.8)		
mean $I/\sigma(I)$	28.1 (6.7)		
Refinement:			
resolution range	42.5−1.20		
no. of protein atoms	2337 (2337)[d]		
number of water molecules	362		
R_{cryst} (%)	14.2		
R_{free} (%)	16.7		
RMS[c] deviations from ideal stereochemistry:			
bond lengths (Å)	0.008		
bond angles (deg)	1.366		
planes (Å)	0.008		
chiral center restraint (Å^3)	0.086		
mean B factor (all atoms) (Å^2)	13.78		
Ramachandran plot:			
favored region (%)	98.1		
allowed regions (%)	1.9		
outlier regions (%)	0.0		

[a]Data in parentheses are statistics for the highest resolution shell. [b]Unique reflections above 3σ. [c]RMS: root-mean square. [d]Atoms with aniso_U.

in the CTX-M-1/3 subgroup, as well as CTX-M-96. These observations could indicate that, although CTX-M family displays a high degree of overall conservation, there are some local differences within the active site that could be possibly associated with minor modifications in the kinetic behavior toward some antibiotics between different CTX-M subgroups.

Reduced Breadth of the CTX-M-96 Active Cavity Is the Result of a Shift of Ω-Loop's Position. As other class A β-lactamases, the active site motifs in CTX-M-96 are located in the interface between the "all α" and "α/β" domains. They are defined as "Ser70-Thr71-Ser72-Lys73" (motif 1, carrying the nucleophile serine), "Ser130-Asp131-Asn132" (motif 2, in the loop between α4 and α5), and "Lys234-Thr235-Gly236" (motif 3, on strand β3), and the 16-residues-long Ω-loop, from Arg164 to Asp179 (Figure 1).

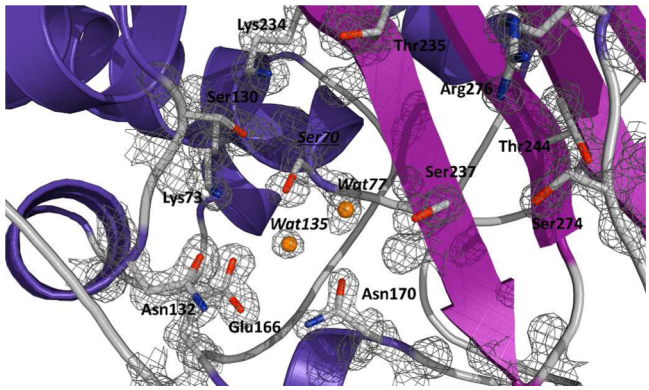

Figure 1. $2F_0 - F_c$ map contoured at 1.5σ is shown in gray around the most important amino acid residues within the active site; oxyanion and deacylating water molecules are shown as orange spheres (Wat77 and Wat135, respectively, according to the PDB numbering).

The structure of the active site includes the most important amino acid residues and the two catalytic water molecules, the oxyanion water (OAW) and the deacylating water (DW), located at conserved position in class A β-lactamases, and all together create the hydrogen bonds network for stabilization of the catalytic pocket (Figure 2).

It is known that both TEM- and SHV-type ESBLs present a widened active site as a result from substitutions in key residues like those at position 238, 164, or 179. These substitutions lead to conformational modifications in the Ω loop and the β3-strand, and the broader active site potentially facilitates the binding of bulkier cephalosporins, including ceftazidime.[11,54]

Compared to these ESBLs, the breadth of the active site seems to be reduced in CTX-M-96, due to a 0.6−2 Å shift (depending on the β-lactamase) upward of the Ω loop's backbone (Figure 3), which is also noticed in TOHO-1 (CTX-M-44) β-lactamase (PDB: 1IYO). This shift of the Ω loop toward the active site serine is expected to work in coordination with other conformational modifications in the architecture of

Table 4. Root-Mean Square Deviations (in Å) between Secondary Structures, Conserved Motifs and Variable Regions of CTX-M-96 and Other Class A β-Lactamases

	Region/motif:	Total length	SXXK motif	SDN motif	Ω loop	β3 strand	KTG motif		
enzyme	residues:	28−290	70−73	130−132	164−179	226−240	234−236	Id (%)[b]	PDB code
CTX-M-15		0.257	0.016	0.004	0.088	0.847	0.009	99.2	4HBT
TOHO-1[a]		0.478	0.012	0.029	0.191	0.340	0.037	85.4	1IYS
CTX-M-9		0.523	0.018	0.033	0.286	0.255	0.021	82.3	1YLJ
CTX-M-27		0.499	0.031	0.016	0.219	0.263	0.021	83.1	1YLP
CTX-M-14		0.467	0.016	0.016	0.231	0.215	0.021	82.7	1YLT
CTX-M-16		0.480	0.044	0.043	0.195	0.276	0.037	82.7	1YLW
TEM-1		1.497	0.113	0.036	0.357	1.114	0.111	38.6	1BTL
TEM-30		1.323	0.091	0.110	0.383	0.743	0.085	38.8	1LHY
PER-2		1.742	0.056	0.023	3.469	1.327	0.029	29.2	3ZNW

[a]TOHO-1 is currently known as CTX-M-44 (http://www.lahey.org/studies/other.asp#table1). [b]Id: Amino acid identity.

DOI: 10.1021/acs.biochem.5b00313
Biochemistry 2015, 54, 5072−5082

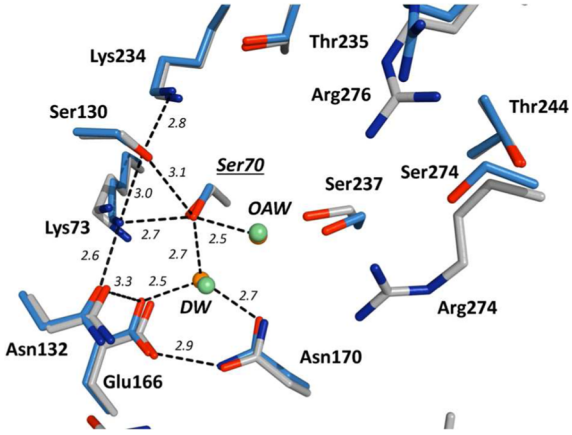

Figure 2. Comparative active site organization of CTX-M-96 (marine blue) and TOHO-1 (gray), indicating the main hydrogen bonds (black dashed lines) implicated in the stabilization of the active site of CTX-M-96. References: oxyanion water (OAW), deacylating water (DW) molecules (orange for CTX-M-96 and green for TOHO-1). For visual convenience, only the hydrogen bonds for CTX-M-96 were shown. Other color references: oxygen (red), nitrogen (blue), sulfur (green). All distances are in angstroms (Å).

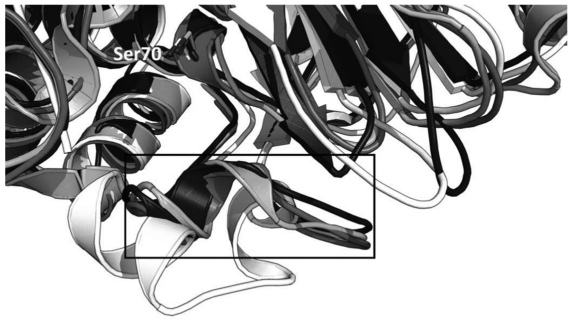

Figure 3. Structural superposition of different β-lactamases showing the differences in the breadth of the active sites (box), mainly due to shifts in the Ω loop. Reference colors: TEM-1 (dark gray; PDB: 1BTL), extended-spectrum TEM-72 (light gray; PDB 3P98), extended-spectrum PER-2 (white; PDB: 4D2O), CTX-M-96 (black).

the catalytic site in order to allow the proper accommodation of bulkier substrates like the oxyimino-cephalosporins.

There is also a hydrogen bond between Asn170O and Asp/Gly240N at the entrance of the active site, range 2.7−2.9 Å, highly conserved in other class A apo-β-lactamases, which has been suggested to be disrupted upon entrance of cefotaxime and ceftazidime. In addition, the presence of the Asp240Gly substitution in CTX-M-96 apparently allows a ca. 0.5 Å shift away from the active-site cleft in the vicinity of position 240, located at the C-terminus of β3 strand.

Simulated Interaction of CTX-M-96 with Oxyimino-Cephalosporins Does Not Seem to Be Conclusive for the "Ceftazidimase" Behavior. In order to correlate the observed phenotypic and kinetic behavior due to the activity of CTX-M-96 (harboring Asp240Gly substitution) with structural evidence drawn from the crystallographic structure of *apo* CTX-M-96, simulated models of the β-lactamase in association with oxyimino-cephalosporins cefotaxime and ceftazidime were obtained using the structure of CTX-M-96 and acyl-enzymes structures of TOHO-1.

By analyzing the model of CTX-M-96 with both cefotaxime (Figure 4) and ceftazidime (Figure 5), we could assess that their interaction with CTX-M-96 could be as favored as with TOHO-1, following overall similar interaction patterns through favored hydrogen bonds and others that could occur if the rotameric conformation of some residues favors them. This stabilizing hydrogen bond network involves important residues like Ser130, Lys234, Thr235, and Ser237, and others like Asn104, Asn132, and Asn170.

Compared to the structure of TOHO-1 acylated by both cefotaxime and ceftazidime (PDB: 1IYO and 2ZQD), cephalosporin molecules seem to lie slightly rotated within the active site in the models of CTX-M-96, partly due to different positioning of some amino acid rotamers and the deacylating water (DW) molecule. For ceftazidime, the bulkier carboxy-propoxyimino group at C7 could be also oriented, although probably after a slowed entry to the active site, reflected by the normally low affinity values observed (K_M > 1 mM; Table 2), which is common to all CTX-M enzymes.

Also, after comparison with structures of CTX-M-9 and CTX-M-14 in complex with oxyimino-cephalosporins (PDB: 3HLW, 1YLY, and 1YLZ), residues like Asn132, Glu166, Pro167, and Asn170 appear to be shifted up to 0.7 Å away from the catalytic cleft in the *apo* CTX-M-96 structure, suggesting that the presence of antibiotic induces the approach of these residues toward the cephalosporin through stabilizing hydrogen

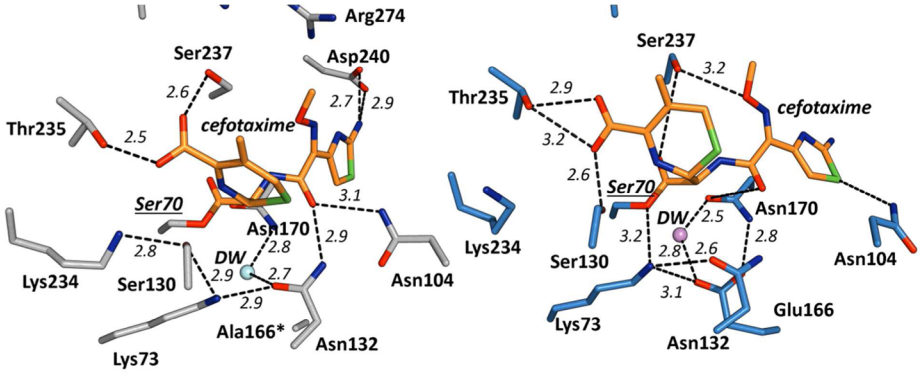

Figure 4. Detailed view of the active site of TOHO-1 in association with cefotaxime (left panel), indicating the main hydrogen bonds interactions (PDB entry: 1IYO), and simulated modeling of CTX-M-96 and the probable positioning of cefotaxime within the active site (right panel), suggesting the putative most favorable hydrogen bonds for the stabilization of the oxyimino-cephalosporin molecule; TOHO-1 contains Glu166Ala mutation (marked with an asterisk). All distances are in angstroms (Å).

DOI: 10.1021/acs.biochem.5b00313
Biochemistry 2015, 54, 5072−5082

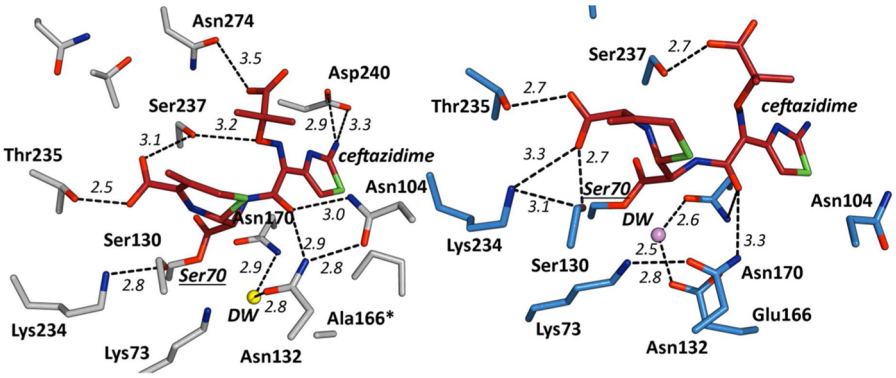

Figure 5. Active site of TOHO-1 in complex with acylated ceftazidime (left panel), indicating the main hydrogen bonds (PDB entry: 2ZQD), compared to a simulated model of CTX-M-96 and its probable association with ceftazidime (right panel), showing the predicted positioning of the molecule and the hydrogen bonds interactions. Other color references: oxygen (red), nitrogen (blue), sulfur (green), cefotaxime (orange), ceftazidime (purple). All distances are in angstroms (Å).

bonds, in agreement with the models of CTX-M-96 in complex with these antibiotics (not shown).

Finally, it is possible that the entry of both oxyimino-cephalosporins to the active site also involves the disruption of the hydrogen bond between residues 170−240, as suggested for CTX-M-9 and cefotaxime;[54] the distance between the Asn170O and Gly240N in CTX-M-96 is shorter (2.9 Å) than that resulting from the accommodation of the cephalosporin into the active site of variants like CTX-M-9 and TOHO-1 (up to 3.6 Å), somewhat in agreement with this previous hypothesis.

These findings could be in agreement with the proposed "breathing" of the CTX-M or ligand induced conformational flexibility of CTX-M favored by the Asp240Gly replacement.[18] According to this model, the insertion of the ceftazidime's side chain deep in the catalytic domain, along with a coordinated movement of Ser70, the β3-strand, and the Ω-loop, facilitates the interaction with the antibiotic.

The Asp240Gly Mutation Does Not Appear to Affect the Overall Secondary or Tertiary Structure. In agreement with the crystallographic structure presented herein, the center of mass of the fluorescence emission spectra (342 nm) reveals that Trp residues of CTX-M-96 are placed in a somehow hydrophilic environment (Figure 6a). Additionally, the far UV CD spectrum of native CTX-M-96 in buffer displays two minima at ∼208 and 220 nm, a distinctive feature of a protein with a high α-helical content (47%, according to the X-ray structure) (Figure 6b,c).

Moreover, these results reveal that CTX-M-96 and CTX-M-12 are undistinguishable proteins with regard to their secondary structure and tertiary folding. According to fluorescence emission spectra, both enzymes seem to have an identical center of mass, and the difference in intensities is not relevant.

Therefore, the presence of Gly or Asp at position 240 does not seem to affect the overall structure and folding of the proteins. Nevertheless, a local rearrangement cannot be discarded.

Alterations in Expression of Specific Outer-Membrane Porins Contribute to the Overall Resistance. We evaluated the influence of specific outer-membrane porins in the phenotypic resistance of *E. coli* strains featuring alterations in their expression, after introduction of plasmids harboring the $bla_{\text{CTX-M-12}}$ and $bla_{\text{CTX-M-96}}$ and expressed under isogenic backgrounds. In Table 5, the minimum inhibitory concentrations (MIC) of the oxyimino-cephalosporins cefotaxime and ceftazidime are shown.

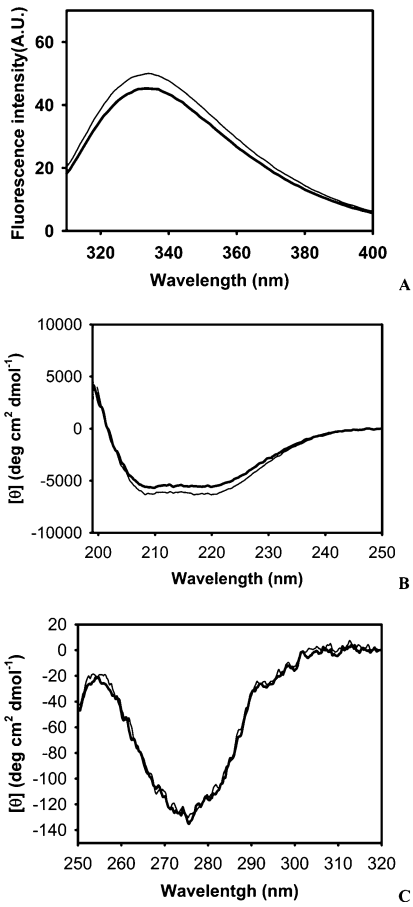

Figure 6. Spectroscopic characterization of CTX-M-96 vs CTX-M-12. Panel A depicts the intrinsic fluorescence emission spectrum. Far and near UV circular dichroism spectra are shown in panels B and C, respectively (bold line: CTX-M-96; thin line: CTX-M-12).

According to our results, the resistance phenotype of all clones (in the presence of CTX-M 12 or the presence of CTX-M96) toward cefotaxime remains invariant (all strains are resistant to this drug). On the other hand, an alteration in OmpC expression yields intermediate resistance toward ceftazidime, while deficiency of OmpF results in resistance to this antibiotic (only in the presence of CTX-M-96). Therefore,

DOI: 10.1021/acs.biochem.5b00313
Biochemistry 2015, 54, 5072−5082

Table 5. Minimum Inhibitory Concentrations (MIC, in $\mu g\ mL^{-1}$) of Oxyimino-cephalosporins for *E. coli* K12 and Derived Isogenic Porin-Defficient Strains Expressing CTX-M-12 and CTX-M-96[a]

		cefotaxime				ceftazidime			
strain	alteration	*b*	pK19	pK12 ($bla_{CTX\text{-}M\text{-}12}$)	pK96 ($bla_{CTX\text{-}M\text{-}96}$)	*b*	pK19	pK12 ($bla_{CTX\text{-}M\text{-}12}$)	pK96 ($bla_{CTX\text{-}M\text{-}96}$)
E. coli K12		≤0.125	≤0.125	64	64	0.06	0.06	2	8
E. coli JF694	$ompC^{-}$ $ompF^{-}$	≤0.125	≤0.125	128	256	0.125	0.125	16	128
E. coli JF700	$ompA^{-}$ $ompF^{-}$	≤0.125	≤0.125	64	128	0.25	0.25	4	64
E. coli JF701	$ompC^{-}$	≤0.125	≤0.125	64	64	≤0.016	≤0.016	0.5	8
E. coli JF703	$ompF^{-}$	≤0.125	≤0.125	256	256	0.25	0.25	8	128

[a]Plasmids: pK19, plasmid vector (Kan^{r}) used for cloning $bla_{CTX\text{-}M\text{-}12}$ and $bla_{CTX\text{-}M\text{-}96}$ genes; pK12 and pK96, plasmids harboring the $bla_{CTX\text{-}M\text{-}12}$ or $bla_{CTX\text{-}M\text{-}96}$ genes cloned at the *Sma*I site of pK19 vector, respectively (see Experimental Procedures section for details). [b]No plasmid was introduced.

alterations in OmpF porin expression seem to be determinant to achieve resistance levels to ceftazidime similar to those observed in clinical isolates producing a CTX-M β-lactamase with the Asp240Gly substitution.

CONCLUSIONS

It has been stated that the expansion of hydrolytic activities of the CTX-M β-lactamases toward the oxyimino-cephalosporins relies on an enhanced mobility of the β3-strand obtained after substitutions like Asp240Gly and Val231Ala, expanding the activity toward ceftazidime, or a direct interaction of specific amino acids (probably Ser237 and Asn104) with the oxyimino side chains of third-generation cephalosporins, and that those substitutions are also correlated with lower stability of the enzyme.[11]

From the discussion on our findings, we postulate that there seem to be subtle changes in the conformation of the active site cavity of CTX-M-96, compared to enzyme variants harboring the Asp240, and these small rearrangements could be due to localized shifts in the environment of the β3 strand. According to the crystallographic evidence, CTX-M-96 presents a "compact" active site, which in spite of its reduced cavity seems to allow the proper interaction with oxyimino-cephalosporins, as suggested by simulated models and previously determined crystallographic structures of other variants (see PDB entries 3HLW, 1YLY, and 1YLZ as examples).

We reinforce herein that structural differences between CTX-M harboring the Asp240Gly mutation (and also probably others like those at Pro167) do not seem to be conclusive to determine the "ceftazidimase" behavior observed *in vivo*, which is in turn partially supported by the mild improvement in the catalytic efficiency toward ceftazidime by CTX-M-96 and similar enzymes, compared to "parental" Asp240-harboring variants. Moreover, mutations at position 167 that lead to large increases in the MICs to ceftazidime for the producing strains also result in only discrete catalytic efficiency improvement toward ceftazidime.[2,8]

We therefore propose that the observed *in vivo* resistance is due to the sum of different mechanisms acting synergistically and not merely a consequence of structural differences. Besides the enzyme's activity, we must also consider the differential permeability of oxyimino-cephalosporins. We are showing that alterations in OmpF expression (and, to a lesser extent, probably OmpC) result in resistance to ceftazidime, even when an enzyme with only a slight improvement in the catalytic efficiency toward this drug, like CTX-M-96, is expressed. These results are supported by previous studies in which the relative permeation of β-lactams through OmpF and OmpC was evaluated.[55,56] In these studies, it was proposed that the strength of the OmpF−oxyimino−cephalosporins interaction follows the order cefotaxime > cefepime > ceftazidime, which is directly associated with the permeation rate through this porin. Also, they showed that OmpF binds the oxyimino-cephalosporins more strongly than OmpC (which also has a narrower channel than OmpF), and this results in a more efficient translocation of these drugs through OmpF than OmpC.

The term "ceftazidimases" that is currently applied for the Asp240Gly-harboring CTX-M variants should be carefully reconsidered. Instead, these β-lactamases should be considered as "cefotaximases associated with ceftazidime resistance", whose slightly improved activity toward ceftazidime acts in concert with other subtle resistance mechanisms, like alterations in OmpF. This combination would be sufficient to shift the MICs of ceftazidime to a clinically significant level.

AUTHOR INFORMATION

Corresponding Author

*Telephone: +54 11 4964 8285. Fax: +54 11 4508 3645. E-mail: ppower@ffyb.uba.ar.

Author Contributions

⊥E.S. and P.P. contributed equally.

Funding

This work was supported by grants from the University of Buenos Aires (UBACyT 20020110200017 to P.P.), Agencia Nacional de Promoción Científica y Tecnológica (BID PICT2011−0742 to G.G.), Fonds de la Recherche Scientifique (IISN 4.4509.11), University of Liège (Fonds spéciaux, Crédit classique, C-09/75 and C-12/38).

Notes

The authors declare no competing financial interest.

ACKNOWLEDGMENTS

P.P., M. M.R., L.C., and G.G. are researchers at the Consejo Nacional de Investigaciones Científicas y Técnicas (CONICET, Argentina). F.K. is a researcher at the Fonds de la Recherche Scientifique (FNRS, Belgium). We thank the staff of Proxima1 beamline at Soleil synchrotron for assistance in X-ray data collection. Additional training and collaborative activities were supported by a bilateral scientific agreement (V4/325C) between the FRS-FNRS to M.G. and the CONICET to P.P.

ABBREVIATIONS

ESBL, extended-spectrum β-lactamase; MIC, minimum inhibitory concentration; CLSI, Clinical and Laboratory Standards Institute; LB, Luria−Bertani culture medium; IPTG, isopropyl-β-D-1-thiogalactopyranoside; SDS-PAGE, sodium dodecyl sulfate polyacrylamide gel electrophoresis; MES, 2-(*N*-

DOI: 10.1021/acs.biochem.5b00313
Biochemistry 2015, 54, 5072−5082

morpholino)ethanesulfonic acid; Tris, 2-amino-2-hydroxymethylpropane-1,3-diol

REFERENCES

(1) Gutkind, G. O., Di Conza, J., Power, P., and Radice, M. (2013) β-Lactamase-mediated resistance: a biochemical, epidemiological and genetic overview. *Curr. Pharm. Des. 19*, 164−208.

(2) Rossolini, G. M., D'Andrea, M. M., and Mugnaioli, C. (2008) The spread of CTX-M-type extended-spectrum β-lactamases. *Clin. Microbiol. Infect. 14*, 33−41.

(3) Canton, R., and Coque, T. M. (2006) The CTX-M β-lactamase pandemic. *Curr. Opin. Microbiol. 9*, 466−475.

(4) Decousser, J. W., Poirel, L., and Nordmann, P. (2001) Characterization of a chromosomally encoded extended-spectrum class A β-lactamase from *Kluyvera cryocrescens*. *Antimicrob. Agents Chemother. 45*, 3595−3598.

(5) Humeniuk, C., Arlet, G., Gautier, V., Grimont, P., Labia, R., and Philippon, A. (2002) β-Lactamases of *Kluyvera ascorbata*, probable progenitors of some plasmid-encoded CTX-M types. *Antimicrob. Agents Chemother. 46*, 3045−3049.

(6) Poirel, L., Kampfer, P., and Nordmann, P. (2002) Chromosome-encoded Ambler class A β-lactamase of *Kluyvera georgiana*, a probable progenitor of a subgroup of CTX-M extended-spectrum β-lactamases. *Antimicrob. Agents Chemother. 46*, 4038−4040.

(7) Rodriguez, M. M., Power, P., Radice, M., Vay, C., Famiglietti, A., Galleni, M., Ayala, J. A., and Gutkind, G. (2004) Chromosome-encoded CTX-M-3 from *Kluyvera ascorbata*: a possible origin of plasmid-borne CTX-M-1-derived cefotaximases. *Antimicrob. Agents Chemother. 48*, 4895−4897.

(8) Bonnet, R. (2004) Growing group of extended-spectrum β-lactamases: the CTX-M enzymes. *Antimicrob. Agents Chemother. 48*, 1−14.

(9) Bradford, P. A. (2001) Extended-spectrum β-lactamases in the 21st century: characterization, epidemiology, and detection of this important resistance threat. *Clin. Microbiol. Rev. 14*, 933−951.

(10) Power, P., Di Conza, J., Rodriguez, M. M., Ghiglione, B., Ayala, J. A., Casellas, J. M., Radice, M., and Gutkind, G. (2007) Biochemical characterization of PER-2 and genetic environment of bla_{PER-2}. *Antimicrob. Agents Chemother. 51*, 2359−2365.

(11) Chen, Y., Delmas, J., Sirot, J., Shoichet, B., and Bonnet, R. (2005) Atomic resolution structures of CTX-M β-lactamases: extended spectrum activities from increased mobility and decreased stability. *J. Mol. Biol. 348*, 349−362.

(12) Ibuka, A. S., Ishii, Y., Galleni, M., Ishiguro, M., Yamaguchi, K., Frere, J. M., Matsuzawa, H., and Sakai, H. (2003) Crystal structure of extended-spectrum β-lactamase Toho-1: insights into the molecular mechanism for catalytic reaction and substrate specificity expansion. *Biochemistry 42*, 10634−10643.

(13) Cartelle, M., del Mar Tomas, M., Molina, F., Moure, R., Villanueva, R., and Bou, G. (2004) High-level resistance to ceftazidime conferred by a novel enzyme, CTX-M-32, derived from CTX-M-1 through a single Asp240-Gly substitution. *Antimicrob. Agents Chemother. 48*, 2308−2313.

(14) Bae, I. K., Lee, B. H., Hwang, H. Y., Jeong, S. H., Hong, S. G., Chang, C. L., Kwak, H. S., Kim, H. J., and Youn, H. (2006) A novel ceftazidime-hydrolysing extended-spectrum β-lactamase, CTX-M-54, with a single amino acid substitution at position 167 in the omega loop. *J. Antimicrob. Chemother. 58*, 315−319.

(15) Bonnet, R., Dutour, C., Sampaio, J. L., Chanal, C., Sirot, D., Labia, R., De Champs, C., and Sirot, J. (2001) Novel cefotaximase (CTX-M-16) with increased catalytic efficiency due to substitution Asp-240– > Gly. *Antimicrob. Agents Chemother. 45*, 2269−2275.

(16) Bonnet, R., Recule, C., Baraduc, R., Chanal, C., Sirot, D., De Champs, C., and Sirot, J. (2003) Effect of D240G substitution in a novel ESBL CTX-M-27. *J. Antimicrob. Chemother. 52*, 29−35.

(17) Poirel, L., Gniadkowski, M., and Nordmann, P. (2002) Biochemical analysis of the ceftazidime-hydrolysing extended-spectrum β-lactamase CTX-M-15 and of its structurally related β-lactamase CTX-M-3. *J. Antimicrob. Chemother. 50*, 1031−1034.

(18) Delmas, J., Chen, Y., Prati, F., Robin, F., Shoichet, B. K., and Bonnet, R. (2008) Structure and dynamics of CTX-M enzymes reveal insights into substrate accommodation by extended-spectrum β-lactamases. *J. Mol. Biol. 375*, 192−201.

(19) Antunes, N. T., Frase, H., Toth, M., Mobashery, S., and Vakulenko, S. B. (2011) Resistance to the third-generation cephalosporin ceftazidime by a deacylation-deficient mutant of the TEM β-lactamase by the uncommon covalent-trapping mechanism. *Biochemistry 50*, 6387−6395.

(20) Goessens, W. H., van der Bij, A. K., van Boxtel, R., Pitout, J. D., van Ulsen, P., Melles, D. C., and Tommassen, J. (2013) Antibiotic trapping by plasmid-encoded CMY-2 β-lactamase combined with reduced outer membrane permeability as a mechanism of carbapenem resistance in *Escherichia coli*. *Antimicrob. Agents Chemother. 57*, 3941−3949.

(21) Levitt, P. S., Papp-Wallace, K. M., Taracila, M. A., Hujer, A. M., Winkler, M. L., Smith, K. M., Xu, Y., Harris, M. E., and Bonomo, R. A. (2012) Exploring the role of a conserved class A residue in the Omega-Loop of KPC-2 β-lactamase: a mechanism for ceftazidime hydrolysis. *J. Biol. Chem. 287*, 31783−31793.

(22) Kimura, S., Ishiguro, M., Ishii, Y., Alba, J., and Yamaguchi, K. (2004) Role of a mutation at position 167 of CTX-M-19 in ceftazidime hydrolysis. *Antimicrob. Agents Chemother. 48*, 1454−1460.

(23) Novais, A., Comas, I., Baquero, F., Canton, R., Coque, T. M., Moya, A., Gonzalez-Candelas, F., and Galan, J. C. (2010) Evolutionary trajectories of β-lactamase CTX-M-1 cluster enzymes: predicting antibiotic resistance. *PLoS Pathog. 6*, e1000735.

(24) Bush, K., Jacoby, G. A. Updated functional classification of β-lactamases, *Antimicrob. Agents Chemother.* 201054, 969−976.10.1128/AAC.01009-09

(25) Villegas, M. V., Correa, A., Perez, F., Zuluaga, T., Radice, M., Gutkind, G., Casellas, J. M., Ayala, J., Lolans, K., and Quinn, J. P. (2004) CTX-M-12 β-lactamase in a *Klebsiella pneumoniae* clinical isolate in Colombia. *Antimicrob. Agents Chemother. 48*, 629−631.

(26) Clinical and Laboratory Standards Institute. (2013) *Performance Standards for Antimicrobial Susceptibility Testing*; twenty-third informational supplement M100-S22, Clinical and Laboratory Standards Institute, Wayne, PA, USA.

(27) Foulds, J., and Chai, T. (1979) Isolation and characterization of isogenic *E. coli* strains with alterations in the level of one or more major outer membrane proteins. *Can. J. Microbiol. 25*, 423−427.

(28) Hansen, J. B., and Olsen, R. H. (1978) Isolation of large bacterial plasmids and characterization of the P2 incompatibility group plasmids pMG1 and pMG5. *J. Bacteriol. 135*, 227−238.

(29) Pridmore, R. D. (1987) New and versatile cloning vectors with kanamycin-resistance marker. *Gene 56*, 309−312.

(30) Power, P., Radice, M., Barberis, C., de Mier, C., Mollerach, M., Maltagliatti, M., Vay, C., Famiglietti, A., and Gutkind, G. (1999) Cefotaxime-hydrolysing β−lactamases in *Morganella morganii*. *Eur. J. Clin. Microbiol. Infect. Dis. 18*, 743−747.

(31) Segel, I. H. (1975) *Enzyme Kinetics, Behavior and Analysis of Rapid Equilibrium and Steady-State Enzyme Systems*; John Wiley & Sons, Inc., New York.

(32) De Meester, F., Joris, B., Reckinger, G., Bellefroid-Bourguignon, C., Frere, J. M., and Waley, S. G. (1987) Automated analysis of enzyme inactivation phenomena. Application to β-lactamases and DD-peptidases. *Biochem. Pharmacol. 36*, 2393−2403.

(33) Papp-Wallace, K. M., Bethel, C. R., Distler, A. M., Kasuboski, C., Taracila, M., and Bonomo, R. A. (2010) Inhibitor resistance in the KPC-2 β-lactamase, a preeminent property of this class A β-lactamase. *Antimicrob. Agents Chemother. 54*, 890−897.

(34) Power, P., Galleni, M., Ayala, J. A., and Gutkind, G. (2006) Biochemical and molecular characterization of three new variants of AmpC β-lactamases from *Morganella morganii*. *Antimicrob. Agents Chemother. 50*, 962−967.

(35) Kabsch, W. (2010) XDS. *Acta Crystallogr., Sect. D: Biol. Crystallogr. 66*, 125−132.

DOI: 10.1021/acs.biochem.5b00313
Biochemistry 2015, 54, 5072−5082

(36) Kabsch, W. (2010) Integration, scaling, space-group assignment and post-refinement. *Acta Crystallogr., Sect. D: Biol. Crystallogr. 66*, 133−144.
(37) Murshudov, G. N., Vagin, A. A., and Dodson, E. J. (1997) Refinement of macromolecular structures by the maximum-likelihood method. *Acta Crystallogr., Sect. D: Biol. Crystallogr. 53*, 240−255.
(38) Painter, J., and Merritt, E. A. (2006) Optimal description of a protein structure in terms of multiple groups undergoing TLS motion. *Acta Crystallogr., Sect. D: Biol. Crystallogr. 62*, 439−450.
(39) Emsley, P., and Cowtan, K. (2004) Coot: model-building tools for molecular graphics. *Acta Crystallogr., Sect. D: Biol. Crystallogr. 60*, 2126−2132.
(40) *The PyMOL Molecular Graphics System*, 1.5.0.4 ed., Schrödinger LLC, New York.
(41) Notredame, C., Higgins, D. G., and Heringa, J. (2000) T-Coffee: A novel method for fast and accurate multiple sequence alignment. *J. Mol. Biol. 302*, 205−217.
(42) Gouet, P., Robert, X., and Courcelle, E. (2003) ESPript/ENDscript: Extracting and rendering sequence and 3D information from atomic structures of proteins. *Nucleic Acids Res. 31*, 3320−3323.
(43) Shimamura, T., Ibuka, A., Fushinobu, S., Wakagi, T., Ishiguro, M., Ishii, Y., and Matsuzawa, H. (2002) Acyl-intermediate structures of the extended-spectrum class A β-lactamase, Toho-1, in complex with cefotaxime, cephalothin, and benzylpenicillin. *J. Biol. Chem. 277*, 46601−46608.
(44) Padayatti, P. S., Helfand, M. S., Totir, M. A., Carey, M. P., Carey, P. R., Bonomo, R. A., and van den Akker, F. (2005) High resolution crystal structures of the *trans*-enamine intermediates formed by sulbactam and clavulanic acid and E166A SHV-1 β-lactamase. *J. Biol. Chem. 280*, 34900−34907.
(45) Krieger, E., Darden, T., Nabuurs, S. B., Finkelstein, A., and Vriend, G. (2004) Making optimal use of empirical energy functions: force-field parameterization in crystal space. *Proteins: Struct., Funct., Genet. 57*, 678−683.
(46) Krieger, E., Joo, K., Lee, J., Raman, S., Thompson, J., Tyka, M., Baker, D., and Karplus, K. (2009) Improving physical realism, stereochemistry, and side-chain accuracy in homology modeling: Four approaches that performed well in CASP8. *Proteins: Struct., Funct., Genet. 77*, 114−122.
(47) Essmann, U., Perera, L., Berkowitz, M. L., Darden, T., Lee, H., and Pedersen, L. G. (1995) A smooth particle mesh Ewald method. *J. Chem. Phys. 103*, 8577−8593.
(48) Schmid, F. (1989) Spectral methods of characterizing protein conformation and conformational changes., In *Protein Structure: A Practical Approach* (Creighton, T. E., Ed.) IRL, New York.
(49) Bae, I. K., Lee, Y. N., Hwang, H. Y., Jeong, S. H., Lee, S. J., Kwak, H. S., Song, W., Kim, H. J., and Youn, H. (2006) Emergence of CTX-M-12 extended-spectrum β-lactamase-producing Escherichia coli in Korea. *J. Antimicrob. Chemother. 58*, 1257−1259.
(50) Ambler, R. P., Coulson, A. F., Frere, J. M., Ghuysen, J. M., Joris, B., Forsman, M., Levesque, R. C., Tiraby, G., and Waley, S. G. (1991) A standard numbering scheme for the class A β-lactamases. *Biochem. J. 276*, 269−270.
(51) Wilson, A. J. C. (1949) The probability distribution of X-ray intensities. *Acta Crystallogr. 2*, 318−321.
(52) Ghuysen, J. M. (1991) Serine β-lactamases and penicillin-binding proteins. *Annu. Rev. Microbiol. 45*, 37−67.
(53) Ibuka, A., Taguchi, A., Ishiguro, M., Fushinobu, S., Ishii, Y., Kamitori, S., Okuyama, K., Yamaguchi, K., Konno, M., and Matsuzawa, H. (1999) Crystal structure of the E166A mutant of extended-spectrum β-lactamase Toho-1 at 1.8 Å resolution. *J. Mol. Biol. 285*, 2079−2087.
(54) Delmas, J., Leyssene, D., Dubois, D., Birck, C., Vazeille, E., Robin, F., and Bonnet, R. (2010) Structural insights into substrate recognition and product expulsion in CTX-M enzymes. *J. Mol. Biol. 400*, 108−120.
(55) Pages, J. M., James, C. E., and Winterhalter, M. (2008) The porin and the permeating antibiotic: a selective diffusion barrier in Gram-negative bacteria. *Nat. Rev. Microbiol. 6*, 893−903.
(56) Mahendran, K. R., Kreir, M., Weingart, H., Fertig, N., and Winterhalter, M. (2010) Permeation of antibiotics through *Escherichia coli* OmpF and OmpC porins: screening for influx on a single-molecule level. *J. Biomol. Screening 15*, 302−307.

DOI: 10.1021/acs.biochem.5b00313
Biochemistry 2015, 54, 5072−5082